

# Thermal Denaturation of Human $\gamma$ -Interferon. A Calorimetric and Spectroscopic Study<sup>†</sup>

Alejandro Beldarrain,<sup>‡</sup> José Luis López-Lacomba,<sup>§</sup> Gustavo Furrázola,<sup>‡</sup> Daysi Barberia,<sup>‡</sup> and Manuel Cortijo<sup>\*,§</sup>

*Centro de Ingeniería Genética y Biotecnología, Apartado 6162, La Habana, Cuba, and Unidad de RMN, Departamento de Química Física II, Facultad de Farmacia, Universidad Complutense de Madrid, 28040-Madrid, Spain*

*Received February 5, 1999; Revised Manuscript Received April 8, 1999*

**ABSTRACT:** The thermal denaturation of a recombinant human  $\gamma$ -interferon has been studied as a function of pH in the range from 2 to 10 and buffer concentration in the range from 5 to 100 mM by differential scanning calorimetry, circular dichroism, fluorescence, <sup>1</sup>H NMR, and biological activity measurements. The thermal transitions are irreversible at high buffer concentrations at all pH values studied, although they are reversible between pH 3.5 and 5.4 at low buffer concentrations. The denaturation enthalpy,  $\Delta H(T_m)$ , at denaturation temperature  $T_m$  was a function of both  $T_m$  and the buffer concentration, and this resulted in heat capacity changes decreasing with buffer concentration. When the denaturation enthalpies were corrected for  $T_m$  dependence, they did not appear to change versus pH. The denaturation entropies, however, appeared to decrease with pH, leading to a small but appreciable increase in the stability of the protein with pH. The difference between the number of moles of protons stoichiometrically bound to a mole of protein in the native and thermally denatured state,  $\Delta N^D$ , was calculated from the variation of  $T_m$  versus pH at each buffer concentration. The values obtained appear to depend on pH alone rather than upon temperature or buffer concentration, a result which agrees with the invariance of the denaturation enthalpies with pH. This dependence was fitted to the titration curve of a group with a pK of 5.4.

Interferons are small proteins that exert antiviral, antiproliferative, and immunoregulatory activities in a variety of mammalian cells (1). The biologically active forms of  $\gamma$ -interferon are dimers of a single polypeptide chain about 140 amino acid residues long, with no disulfide bridges (2). The X-ray structure of rabbit  $\gamma$ -interferon reveals that each subunit has six helices running almost parallel to the symmetry axis (3–5). NMR studies show a very similar secondary structure in solution (6). The tridimensional structure of human  $\gamma$ -interferon bound to its receptor has also been determined by X-ray diffraction (7). Its core structure generally agrees with the structure of unbound  $\gamma$ -interferon (5). The greatest structural differences occur in the flexible AB loop (residues 18–26), which undergoes a conformational change that includes the formation of a  $3_{10}$  helix upon receptor binding.

Human  $\gamma$ -interferon has been cloned and expressed in *E. coli* in several laboratories (8–12). There are minor sequence differences in these preparations compared to the wild-type form; they are not glycosylated and all have similar biological activity (8, 13–15). The C-terminus in natural human interferon is heterogeneous (13, 16, 17). The only difference

between our sample and that used by Lundell et al. (17) is that ours had a methionine residue at the N-terminus, M1, and a glutamic acid residue at the C-terminus, Q146. Some studies published on the stability of  $\gamma$ -interferon (18–21) focus mainly upon acid unfolding, the consequences of its aggregation, and the effect of some point mutations on its biological activity and receptor recognition. The only study into the thermal inactivation of  $\gamma$ -interferon (22) is almost 10 years old and relied almost entirely on optical absorption measurements. We have therefore made a detailed study into the thermal unfolding of this protein as a function of pH and buffer concentration, using principally differential scanning calorimetry (DSC) and circular dichroism (CD). It should be pointed out at this juncture that DSC is the most direct and accurate technique known today for obtaining information about the stability and thermodynamics of biopolymer structures. Moreover, we have found that the reversibility of the thermal unfolding is highly dependent upon the experimental conditions. A knowledge of the reversibility window is of great practical importance because recombinant  $\gamma$ -interferon is usually obtained in the form of inclusion bodies, which are dissolved at a high urea concentration and then dialyzed to produce the commercial preparation. Therefore, a detailed study of the folding and unfolding processes of recombinant  $\gamma$ -interferon as a function of pH and ionic strength is strongly recommended both to increase the dimer protein yield and to obtain the highest biological activity, apart from any other advantages that might accrue from reaching a deeper understanding of the folding–unfolding reaction of this protein.

<sup>†</sup>This research was supported by the Spanish “Ministerio de Educación y Cultura” (Grants PB91-0368 and BIO95-2068E). A.B. was a fellow of the ICI (Spain).

\* Address correspondence to this author at the Unidad de RMN, Departamento de Química Física II, Facultad de Farmacia, Universidad Complutense de Madrid, 28040-Madrid, Spain. E-mail: cortijo@eucmax.sim.ucm.es. Telephone: +34 91 394 3241. Fax: +34 91 394 3245.

<sup>‡</sup> Centro de Ingeniería Genética y Biotecnología.

<sup>§</sup> Universidad Complutense de Madrid.

## EXPERIMENTAL PROCEDURES

**Protein Purification.** Recombinant DNA-derived human  $\gamma$ -interferon was purified from *E. coli* extracts (11). It had a methionine residue at the N-terminus instead of the pyro-glutamic acid of the wild-type protein and a C-terminus glutamic acid at position 146. It was not glycosylated. The recombinant protein was highly purified (more than 99%) and showed biological activity in the range of  $(1.7\text{--}2.3) \times 10^7$  IU/mg. A molecular weight of 33 780 per dimer was used in this work. The molar extinction coefficient of  $\gamma$ -interferon, at 280 nm in 10 mM sodium phosphate buffer, pH 7.0, was determined from its amino acid composition and its absorbance in that buffer and in 6 M guanidine hydrochloride (23). A value of  $30\,000\text{ M}^{-1}\text{ cm}^{-1}$  was obtained. A specific volume of 0.737 mL/g was calculated from its primary sequence by using the values reported by Makhatadze et al. (24) for the amino acid residues. Practically the same results were obtained using the value of 0.752 mL/g quoted in Arakawa et al. (19).

The purity of the samples was checked by reverse-phase HPLC in a Waters 625 LC chromatographic system, consisting of a quaternary pump 525, a Waters photodiode array detector, and Millennium 2010 chromatographic manager software. The protein was loaded into a  $4.5 \times 150$  mm Nucleosil RP C4 column (Alltech), and a linear gradient of acetonitrile (30–70%, v/v) in a 0.1% (v/v) trifluoroacetic acid solution was applied at a flow rate of 0.7 mL/min. Biological activity was assayed by inhibition of the cytopathic effect on a Hep-2 cell, according to the method described by Nisbet et al. (25). The international reference standard of human interferon used was that designed as Gg 23901-530 by WHO.

The buffers were acetic acid/sodium acetate below pH 6.0 and sodium phosphate at and above pH 6.0, measured at 25 °C and given without any correction unless otherwise indicated. We applied the published protonation enthalpies for these buffers (26) to correct the pH at the  $T_m$  values obtained, and it was found that the corrections were always less than  $-0.1$  unit for the acetate buffers and about  $-0.2$  unit for the phosphate ones (cf. Table 1 and Figure 4).

**Emission Fluorescence, Circular Dichroism, and NMR.** Spectra of  $\gamma$ -interferon under several different experimental conditions were recorded with an SLM fluorometer, a Jasco 710 spectropolarimeter, and a Bruker AMX-500 spectrometer. The sample temperature was maintained during the CD and fluorescence measurements by using a circulating water bath connected to the water-jacketed cell holders. Each CD spectrum was scanned 5 times to increase the signal/noise ratio. The CD spectra were deconvoluted according to the methods published in the literature (27). We preferentially used the CCA method (28). Water suppression in the NMR measurements was achieved by selective presaturation, placing the carrier on the HOD resonance. The temperatures in the NMR experiments were calculated from the OH and CH<sub>2</sub> chemical shifts of an 80% glycol dimethyl sulfoxide-*d*<sub>6</sub> sample.

**Differential Scanning Calorimetry.** Calorimetric experiments were made with a digitally controlled DASM-4 microcalorimeter (29), at heating rates from 0.25 to 2.2 K/min. The measurements are taken with this instrument every 0.1 K, thus allowing fittings to the theoretical equations

with lower statistical uncertainties than when the points are taken every 0.5 K. DSC scans were terminated several degrees above the end of the calorimetric transition to ensure that the post-transition heat capacity levels were adequately defined. Second (reheating) scans were always made after cooling from the first ones. Reversibility (taken as the ratio of the transition areas of the second to the first scan) depended upon the experimental conditions. In some cases it was higher than 95% while in others it was negligible. The apparent  $C_p$  profiles were obtained by subtracting the instrumental base lines from the experimental thermograms. These base lines were obtained by filling both sample and reference cells with buffer. The thermograms were also corrected for the dynamic response of the instrument (29). We detected no effect from the type of buffer, either acetate or phosphate, at any pH between 4.7 and 6.2, the range in which both buffers exert significant buffer capacity.

The denaturation temperatures,  $T_m$ , were a function of the scan rate when the transitions were irreversible, as was to be expected. We observed, however, that this was also true in some cases in which reversibility was very high. We have tested many proteins with this instrument, and this is the first time we have encountered a reversible transition that depends on the scan rate, although this phenomenon has been reported by some other authors for a few other proteins (30, 31). This dependence was not due to the instrument itself and neither could it be explained by its response time (29); the procedure to correct the spectra for this response time was always applied and always represented very small changes, especially at the slower scan rates, where the correction was practically negligible. Thus, we are now engaged in research to clarify this scan-rate dependence.

**Basic Theory.** The partial heat capacity of a protein,  $C_p$ , for a reversible two-state transition corresponds to the sum of two terms: the so-called chemical or “internal” heat capacity of the protein in solution,  $C_p^{\text{in}}$ , and the excess heat capacity of the unfolding reaction,  $C_p^{\text{ex}}$ , given by the expression (32):

$$C_p = C_p^{\text{ex}} + C_p^{\text{in}} = \frac{\Delta H^2 K}{RT^2(1 + K)^2} + \left( C_{p,0} + \frac{K}{1 + K} \Delta C_p \right) \quad (1)$$

where  $C_{p,0}$  is the heat capacity of the protein in the native state and  $\Delta C_p$  is the overall heat capacity change during the denaturation reaction. It can be assumed that both heat capacities follow a linear dependence upon temperature (32):

$$C_{p,0} = a_0 + b_0 T \quad \Delta C_p = \Delta a + \Delta b T \quad (2)$$

The thermodynamic functions: the standard free energy,  $\Delta G^\circ(T)$ , the enthalpy,  $\Delta H(T)$ , and the entropy,  $\Delta S(T)$ , changes, and the equilibrium constant,  $K$ , for a reversible two-state transition were calculated by using the equations:

$$\Delta H(T) = \Delta H(T_m) + \Delta a(T - T_m) + \Delta b(T^2 - T_m^2)/2 \quad (3)$$

$$\Delta S(T) = \frac{\Delta H(T_m)}{T_m} + \Delta a \ln(T/T_m) + \Delta b(T - T_m) \quad (4)$$

$$\Delta G^\circ(T) = \Delta H(T) - T\Delta S(T) = -RT \ln K \quad (5)$$

where the denaturation temperature,  $T_m$ , is defined as being

the temperature at which  $K = 1$ . Three methods can be used to determine the change in the heat capacity function,  $\Delta C_p$ , between the initial and final states: (a) by direct extrapolation in the thermograms of the linear dependencies before and after the transition; (b) by plotting the calorimetric enthalpy versus the denaturation temperature; (c) from the nonlinear fitting of the  $C_p$  experimental data to eqs 1–5. All the values reported in this paper were obtained by using the second method, which usually leads to less uncertainty, although the values obtained by all methods agreed within the bounds of experimental error.

The difference between the number of moles of protons stoichiometrically bound to a mole of protein in the denatured (high temperature) and the native (low temperature) states,  $\Delta_N^D\nu$ , can be obtained from the dependence of  $T_m$  upon pH (33):

$$\Delta_N^D\nu = \Delta H(T_m) [\ln(10) \cdot RT_m^2 \cdot (\partial \text{pH} / \partial T_m)_{m_3}]^{-1} \quad (6)$$

These values change versus pH according to the equation:

$$\Delta_N^D\nu = \Delta\nu_m [1 + \exp(\ln(10)b(\text{pH} - \text{pK}))]^{-1} \quad (7)$$

where  $\Delta\nu_m$  is the maximum value of  $\Delta_N^D\nu$  and  $\text{pK}$  is the pH at which the value of  $\Delta\nu_m/2$  is obtained.

Changes in the protein–buffer preferential interaction parameter ( $\phi_{23}$ ) were calculated by using the equations given by Plaza del Pino and Sánchez-Ruiz (33):

$$\Delta\phi_{23} = \left( \frac{\partial \Delta G^\circ}{\partial c} \right)_{T, \text{pH}} = \frac{\Delta H_m}{T_m} \left( \frac{\partial T_m}{\partial c} \right)_{\text{pH}} \quad (8)$$

where  $c$  is the buffer concentration. Because our solutions were highly diluted, we have used molarity instead of molality.

The nonlinear least-squares fitting of the experimental data to the theoretical equations was made with programs written in IDL (Interactive Data Language, Research Systems Inc., Boulder, CO). Practically identical parameters were obtained with programs written for Sigma-Plot by Dr. V. Filimonov. Whenever possible, global or simultaneous fittings were carried out to decrease the fitting uncertainties. Discrepancies in reproducibility in the enthalpy,  $\Delta H(T_m)$ , and temperature,  $T_m$ , transitions under all experimental conditions (including different protein batches over a 5 year period) were lower than 50 kJ/mol and 1 K, respectively. The reproducibility of independent experiments within any single protein batch was better than 30 kJ/mol for  $\Delta H$  and 0.4 K for  $T_m$  values.

## RESULTS

**Calorimetry.** We have studied the thermal unfolding of a recombinant human  $\gamma$ -interferon in the pH range from 2 to 10 and at buffer concentrations from 5 to 100 mM (Table 1). We did not observe any appreciable thermal effect at pH values below 3, probably because the protein was already unfolded. The DSC transitions of human  $\gamma$ -interferon in 5 and 10 mM buffers are reversible at pH values of between 3.5 and 5.0 (see, for example, in Figure 1 the high reversibility observed at pH 4.4). Nevertheless, reversibility is highly dependent upon the pH and the ionic strength of the medium. In 20 mM buffers, the DSC transitions were only reversible between pH 4 and 5.4 and were irreversible

Table 1: Temperatures and Enthalpies of the DSC Transitions for Human  $\gamma$ -Interferon under Several pH and Buffer Concentration Conditions<sup>a</sup>

buffer concn	pH	$T_m$ (°C)	$\Delta H$ (kJ/mol of dimer)
5 mM	4.1	52.5	523
	4.3	53.9	530
	4.9	57.5	600
	6.6* <sup>b</sup>	60.6	649
10 mM	3.0*	36.0	165
	3.5	40.3	310
	3.8	44.1	375
	3.9	45.9	401
	4.1	50.1	460
	4.3	51.3	486
	4.5	52.5	503
	4.7	53.8	525
	4.9	54.9	547
	5.1	56.0	560
	5.3	56.9	578
	5.8*	58.3	597
	6.6*	59.5	606
	7.8*	60.2	600
20 mM	3.8*	44.6	323
	3.9	47.2	392
	4.1	50.8	438
	4.3	51.8	460
	4.7	54.3	500
	4.9	56.8	518
	5.8*	59.0	548
	6.6*	60.1	560
	7.8*	60.2	562
	8.8*	60.2	554
50 mM	3.9*	45.2	300
	4.1*	46.7	332
	4.3*	48.4	348
	4.9*	54.5	420
	6.6*	60.0	509
100 mM	4.0*	44.3	252
	4.3*	47.7	294
	5.7*	58.3	401
	6.6*	59.7	438
	7.6*	59.1	448

<sup>a</sup> pH values were measured at 25 °C and corrected to the  $T_m$  values as indicated under Experimental Procedures. <sup>b</sup> Asterisks indicate that reversibility was less than 40% after 2 h of cooling.

in 50 or 100 mM buffers at all pH values studied. Samples of human  $\gamma$ -interferon were heated for 5 min at temperatures just above the DSC transition and cooled for 2 h; their biological activity was then compared with that measured at the same temperature with the same sample before heating. The following percentages of activity recovered were obtained: 82% at pH 4.5, 77% at pH 5.0, and 0% at pH 7.0, all of which agree with the calorimetric results. The concentration of the protein between 0.8 and 2.3 mg/mL had no influence on either the enthalpy,  $\Delta H(T_m)$ , or the temperature of the transition,  $T_m$  (cf. Figure 1). An additional, irreversible, exothermal peak was observed at higher temperatures (with a  $T_m$  about 76 °C) and protein concentrations between 5 and 10 mg/mL in a 10 mM acetate buffer, pH 4.4, which may be due to an aggregation process.

The effect of pH on the thermal transitions observed in 10 mM buffers is plotted in Figure 2. It can be seen that both the enthalpy and the temperature of the transition increased with pH, while the heat capacities for the native and the denatured states apparently merged together, within experimental uncertainty. Therefore, we fitted all the melting

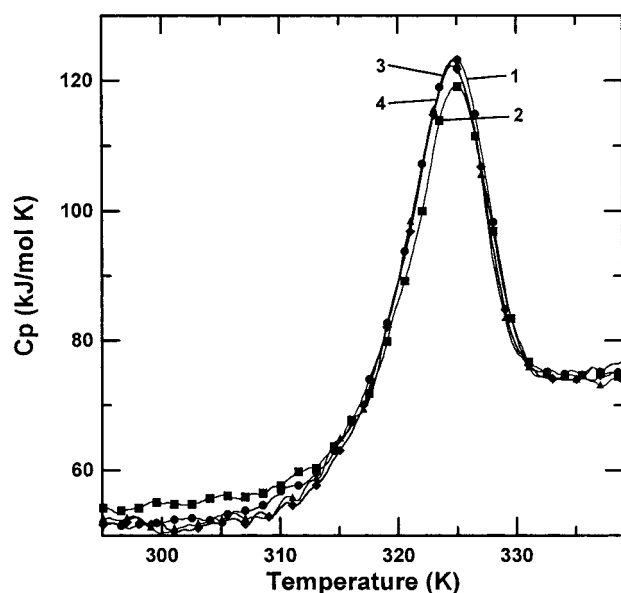


FIGURE 1: Temperature dependence of the apparent heat capacity of recombinant human  $\gamma$ -interferon at 2.10 K/min in a 10 mM acetate buffer, pH 4.4, at the following protein concentrations: curve 1 (●) 2.3 mg/mL; curve 2 (■) reheating of the same sample after cooling it inside the calorimeter cell; curve 3 (◆) 1.2 mg/mL; curve 4 (▲) 0.80 mg/mL.

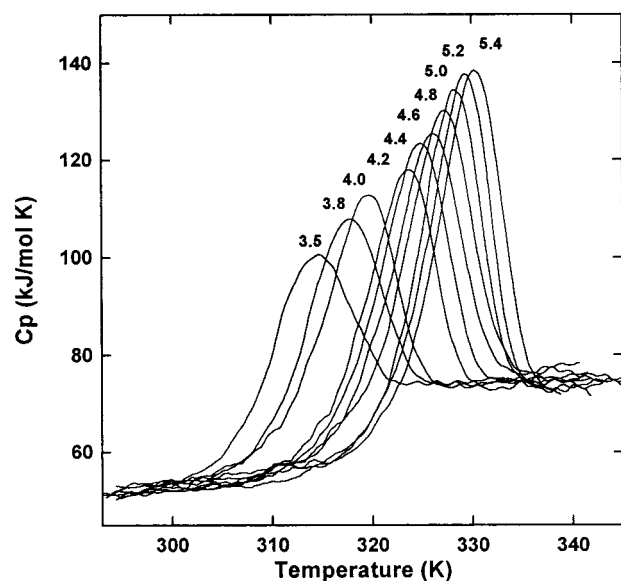


FIGURE 2: pH dependence of the apparent heat capacity-temperature profiles for recombinant human  $\gamma$ -interferon in 10 mM buffers at the indicated pH values. The protein concentrations were about 1.3 mg/mL.

curves simultaneously to eqs 1–5 (cf. Basic Theory section), thus obtaining the temperatures and enthalpies given in Table 1. Similar calculations were made at other buffer concentrations, and the resulting values are also given in Table 1.

Given the small temperature range covered, the relationship between the enthalpies and temperatures of the transition can be fitted to straight lines (Figure 3). We observed a variation in the slopes of the line (i.e., the  $\Delta C_p$  values) versus the buffer concentration, although any direct observation in the thermograms of these changes was precluded due to experimental uncertainty. Nevertheless, the value measured directly from the calorimetric traces [ $15.3 \pm 3.0$  kJ/(mol·K)] agrees with the values plotted in the inset of Figure 3. It can

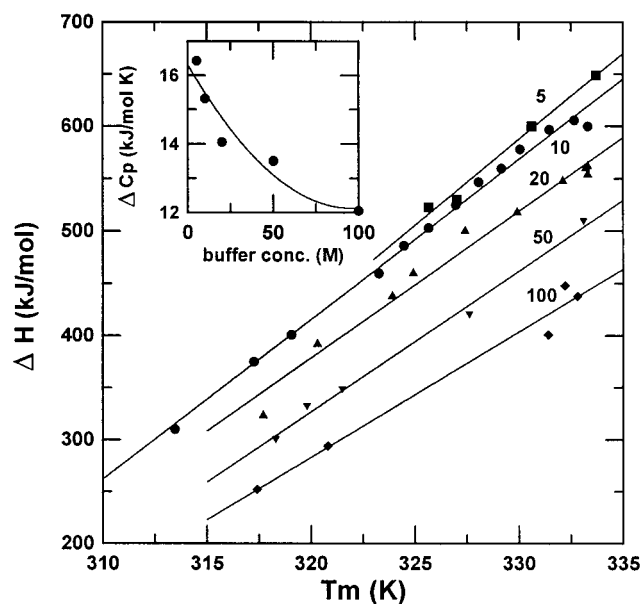


FIGURE 3: Thermal transition enthalpies of human  $\gamma$ -interferon as a function of the transition temperatures,  $T_m$ , under the conditions studied in this work. The symbols stand for the experimental values at the indicated buffer concentrations (mM). The solid lines are the linear least-squares fitted lines, with the slopes,  $\Delta C_p$ , plotted in the inset.

also be seen in the same figure that the denaturation enthalpy is not only a function of  $T_m$  [a fact often observed in the literature (cf. Privalov (34), for example)] but also depends on buffer concentration. So we may well be able to evaluate the difference in the protein–buffer interaction parameter,  $\phi_{23}$ , between the native and unfolded states, as a measure of the mutual perturbation of the chemical potentials of protein and buffer in these states (see below).

Figure 4 shows the profiles of  $T_m$  versus pH for the thermal denaturation of recombinant human  $\gamma$ -interferon at the buffer concentrations studied in this work. The solid lines in the figure represent the best fittings of the experimental data to polynomials and have no theoretical meaning. The derivatives  $(\partial pH / \partial T_m)_c$  at each buffer concentration were obtained from these adjusted polynomial equations. The values of  $\Delta_N^D \nu$  for each pH and buffer studied were obtained from these derivatives and the corresponding  $\Delta H$  values (see Table 1) by using eq 6. The calculated values of the difference between the number of protons bound in the native and the thermally unfolded state per protein dimer are given in the inset of Figure 4. Within the bounds of experimental uncertainty, they seem to define a common pH dependence, indicating that  $\Delta_N^D \nu$  probably depends neither upon buffer concentration nor on temperature. The calculated value of pK (5.4) is close to that which Mulkerrin and Wetzel (22) found to be responsible for the aggregation of wild-type  $\gamma$ -interferon when denatured by heat. Once the change in the number of protons during denaturation is known, it is possible to evaluate the contribution of the protonation enthalpy of the buffer to the unfolding enthalpies measured; this contribution was always smaller than 6 kJ/mol, which is significantly lower than the reproducibility of our measurements, and therefore was always ignored.

The transition temperatures,  $T_m$ , at each pH are lower at higher buffer concentrations, as shown in Figure 4, and thus the values of  $(\partial T_m / \partial c)_{pH}$  are negative. The narrow experi-



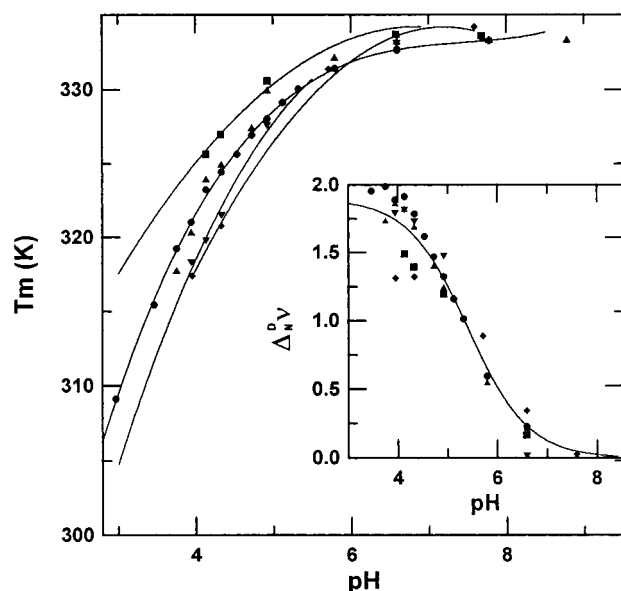


FIGURE 4: Changes in the transition temperatures of human  $\gamma$ -interferon versus pH and buffer concentration. The pH values are corrected to the  $T_m$  values as indicated under Experimental Procedures. The solid lines are the best fittings to polynomials and have no theoretical meaning, although they have been used to calculate  $(\partial T_m / \partial \text{pH})_c$  and the corresponding values of  $\Delta G^{\text{D}}_N$  plotted in the inset. The symbols are equal to those used in Figure 3. Inset:  $\Delta G^{\text{D}}_N$  values were calculated as indicated in the text as a function of pH. The solid line in the inset is the theoretical line described by eq 7 and the values  $\Delta v_m = 1.90 \pm 0.36$ ,  $b = 0.72 \pm 0.33$ , and  $\text{p}K = 5.40 \pm 0.64$ , obtained from the nonlinear fitting.

mental range of buffer concentrations in which the denaturation of this protein is reversible leads to equally small changes in  $T_m$  (less than 6 K), and therefore the experimental errors for these partial derivatives are high. This fact, together with the effect of irreversibility on  $T_m$  at the two higher buffer concentrations, makes it difficult to determine these derivatives with any great accuracy, although they are relatively high [several hundred  $\text{K L (mol of dimer)}^{-1}$ ]. The transition entropies,  $\Delta S(T_m)$ , are about  $1 \text{ kJ K}^{-1} \text{ mol}^{-1}$  positive, and the  $\Delta\phi_{23}$  values are negative, at around several hundred  $\text{kJ L mol}^{-2}$  (cf. eq 8). Another evaluation of  $\Delta\phi_{23}$  may be made from the variation in the denaturation  $\Delta G^\circ$  values versus the buffer concentration using this same eq 8. The values calculated by both methods are negative between 30 and 60  $^\circ\text{C}$ , but the quantitative differences between them are very large (about  $100 \text{ kJ L mol}^{-2}$ ). Therefore, whatever the calculation method used, these values contain large uncertainties, and only general tendencies should be inferred from them. The variations in  $\Delta\phi_{23}$  with temperature appear to have positive slopes at high temperatures whatever the concentration of the buffer. One possible explanation for the negative  $\Delta\phi_{23}$  values might be that the buffer solvates the denatured state more than the native one, thus excluding water molecules from the first solvating layer in the unfolded protein. We must admit, however, that the particular molecular mechanism involved in such a buffer-induced alteration remains unclear.

The change in the standard Gibbs energy function,  $\Delta G^\circ$ , for the unfolding process in the 10 mM buffer as a function of temperature is given in Figure 5, in which it can be seen that the maximum  $\Delta G^\circ$  values are between 9 and 32 kJ/mol

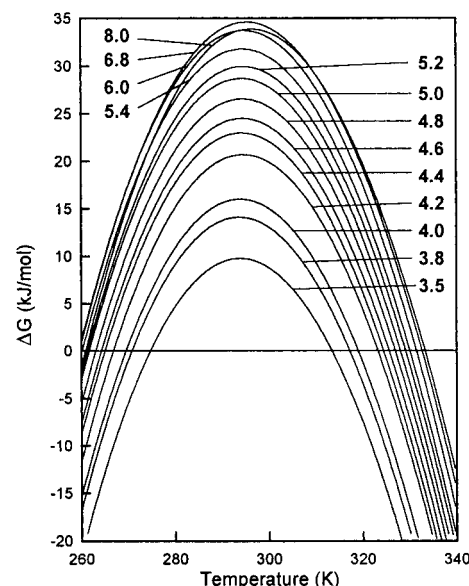


FIGURE 5: Temperature dependence of the Gibbs energy for the thermal unfolding of human  $\gamma$ -interferon in 10 mM buffers at the pH values indicated.

of dimer and correspond to temperatures of about  $26 \pm 4$   $^\circ\text{C}$  at all pH values, stability increasing with pH, as also happens with the  $T_m$  values. These standard Gibbs energy values are of the same order of magnitude as those obtained at other buffer concentrations and for the thermal unfolding of many other proteins (34, 35). The thermodynamic parameters calculated for the unfolding of human  $\gamma$ -interferon at 25  $^\circ\text{C}$  under all our experimental conditions are given in Table 2. It is noteworthy that the uncertainties in  $\Delta H$  and  $\Delta S$  due to the extrapolation method used are very sensitive to small errors in the  $\Delta C_p$  values. Nevertheless, it appears that the denaturation enthalpy remains more or less constant throughout the whole pH range studied, clearly indicating that the decrease in the transition enthalpies versus pH reflected in Table 1 is due to a decrease in the transition temperatures, at least until pH 3.8. This result was to be expected since ionization enthalpies should be very small, and it also agrees with the fact that the  $\Delta G^{\text{D}}_N$  values depend on pH alone and not upon temperature (cf. Figure 4 and eq 9 given in ref 33). It also appears that the denaturation entropies decrease along with an increase in pH (beyond what may be reasonably put down to experimental error), thus explaining the higher protein stability observed at neutral pH. The  $\Delta G^\circ$  values contain fewer uncertainties than  $\Delta H$  and  $\Delta S$ , probably due to a compensation of errors, and are in some cases practically equal to those values determined by other methods (36–39). Maximum stability was found at neutral pH and the lowest buffer concentration used; this represents a value of  $130 \text{ J (mol of res)}^{-1}$ , which is one of the lowest values for protein stability reported in the literature (34, 40, 41). It is worth remembering that this recombinant  $\gamma$ -interferon is not glycosylated, and there is considerable evidence in the literature to suggest that carbohydrate strings usually provide great stability to proteins (42, 43).

**Spectroscopy.** Circular dichroism spectra of recombinant human  $\gamma$ -interferon were registered at 20  $^\circ\text{C}$  as a function of pH. The results are plotted in Figure 6, in which it can be seen that the protein is denatured under acidic conditions, as it is by heat. Deconvolution of the CD spectra leads to

Table 2: Thermodynamic Parameters for the Thermal Unfolding of Recombinant Human  $\gamma$ -Interferon at 25 °C

buffer concn	pH	$\Delta H$ (kJ/mol of dimer)	$T\Delta S$ (kJ/mol of dimer)	$\Delta G^\circ$ (kJ/mol of dimer)
5 mM	4.2	71.2	46.7	24.5
	4.4	56.0	30.8	25.2
	5.0	66.9	35.0	31.8
	6.8	64.9	28.1	36.9
10mM	3.5	75.6	66.3	9.3
	3.8	82.4	68.8	13.6
	4.0	80.8	65.3	15.5
	4.2	75.5	55.1	20.4
	4.4	83.1	60.5	22.6
	4.6	81.7	57.5	24.2
	4.8	83.8	57.6	26.2
	5.0	88.9	60.6	28.3
	5.2	85.1	55.4	29.6
	5.4	89.3	57.8	31.5
	6.0	86.8	53.4	33.5
	6.8	77.5	43.0	34.4
20mM	8.0	61.5	27.7	33.8
	3.8	48.3	37.1	11.3
	4.0	80.8	64.7	16.1
	4.2	76.2	56.2	20.0
	4.4	84.2	62.2	22.0
	4.8	89.0	63.3	25.7
	5.0	71.9	44.3	27.7
	6.0	71.0	40.2	30.8
50mM	6.8	67.6	35.5	32.1
	8.0	68.1	35.9	32.3
	9.0	60.1	28.7	31.4
	4.0	27.8	17.6	10.2
	4.2	39.5	27.2	12.3
100mM	4.4	32.5	19.0	13.5
	5.0	22.1	2.8	19.3
	6.8	36.8	9.1	27.7
	4.0	19.9	11.8	8.1
	4.4	20.8	10.0	10.9
	5.8	0.0	-19.4	19.4
	6.8	20.1	-2.9	23.1
	7.8	37.4	13.2	24.1

the values given in Table 3. Our values at pH 6.8 are not very different from those reported for this protein by Hsu and Arakawa (18) in 0.1 M ammonium acetate (40% helix and 20%  $\beta$  structure) or those calculated from the X-ray structure determined by Earlick et al. (5). We see that the values for antiparallel  $\beta$ -sheets and the aromatic contributions do not change very much with pH. The  $\alpha$ -helix,  $\beta$ -turn, and/or parallel  $\beta$ -sheet contents decrease substantially below pH 4, with a concomitant increase in the nonorganized structures, thus confirming the acid denaturation of the protein.

The near-UV CD spectrum of human  $\gamma$ -interferon disappears at 60 °C (see Figure 7). The tertiary structure is recovered by cooling for 2 h at those pH values at which the calorimetric transitions were reversible. For example, we can see in Figure 7 that the near-UV CD signal returns at pH 4.4, but not at pH 3.0 or 5.0. The secondary structure at pH 5.0, which was also lost by heating, is however almost recovered by cooling, as is shown in the figure. This difference may well be explained by the lower protein concentration used in this latter case, compared to that used for the DSC or near-UV CD experiments. This was confirmed by fluorescence, where we used protein concentrations of about 0.1 mg/mL and could also see reversibility at pH 5.0. It is also shown in Figure 7 that the loss of secondary structure at pH 3.0 is irreversible but that it is reversible at

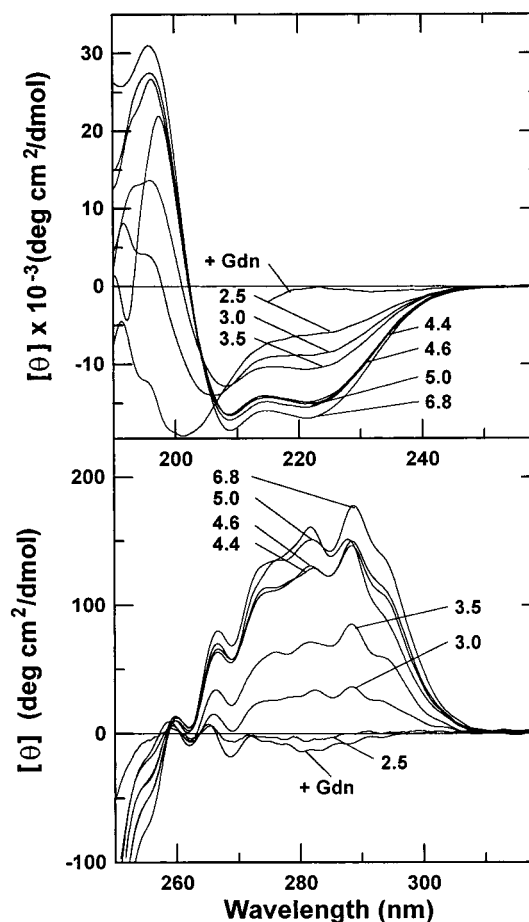


FIGURE 6: CD spectra of  $\gamma$ -interferon at 20 °C in 10 mM buffers at the pH values indicated. The spectrum marked +Gdn was obtained at pH 4.4 and has 6 M guanidine hydrochloride added. The protein concentrations were 0.16 and 1.6 mg/mL for the far-UV and near-UV, respectively.

pH 4.4. Similar conclusions can be drawn from the relative contents of the several structures given in Table 3. We also see that the  $\alpha$ -helix,  $\beta$ -turn, and/or parallel  $\beta$ -sheet contents decrease substantially when the protein is heated and that there is a concomitant increase in the nonordered structures, as also occurs with acid denaturation. Moreover, these facts, together with the values given in Table 3, appear to indicate that the secondary structure in both denatured states (by heat and by acid) is similar, although it is generally accepted that CD is unable to detect small conformational changes.

The fluorescence spectra of  $\gamma$ -interferon at pH values between 4 and 7 at 25 °C show an emission maximum at 336 nm by excitation at 290 nm, which is due to its single tryptophan residue at position 37. Heating at pH 4–5 causes a red shift with a maximum at 346 nm, which reverts to 336 nm by cooling and which agrees with the calorimetric, biological activity, and CD results shown above. At higher pH values, equal changes brought about by heating are irreversible, as was also shown by the other techniques.

$^1\text{H}$  NMR spectra of human  $\gamma$ -interferon in  $\text{D}_2\text{O}$  under several conditions are shown in Figure 8. At pH 4.4 (Figure 8A), the presence of several high-field methyl resonances and the dispersion of the aromatic protons indicate a well-defined tertiary structure, which is also observed in the heated samples after cooling (Figure 8B). We also observed some signals due to amide protons, indicating that some of them

Table 3: Secondary Structure of Recombinant Human  $\gamma$ -Interferon Obtained from the CD Spectra, As Described under Experimental Procedures

pH	$\alpha$ -helix	$\beta$ -turns and parallel $\beta$ -sheet	antiparallel $\beta$ -sheet	aromatic contributions	nonorganized structure
Measured at 20 °C					
2.5	2.5	1.4	10.1	10.6	75.3
3.0	16.0	6.8	9.9	16.5	50.9
3.5	20.9	16.6	14.7	16.2	31.4
4.4	30.8	32.2	10.6	11.4	15.0
4.6	32.0	33.0	10.1	12.1	12.5
5.0	19.5	48.3	16.5	2.5	16.2
6.8	34.6	40.8	7.7	8.4	8.5
Measured at 70 °C					
2.5	0.3	6.7	14.9	3.8	74.4
3.0	4.4	—	16.3	13.8	65.5
3.5	7.2	1.5	—	15.2	63.0
4.4	10.8	7.0	11.4	10.9	60.0
4.6	12.7	8.4	12.5	11.3	55.1
5.0	7.4	15.8	17.3	11.6	47.9
6.8	3.3	—	38.6	23.0	35.1
Sample Heated at 70 °C and Measured at 20 °C after 2 h Cooling					
2.5	—	—	—	—	—
3.0	11.7	8.8	6.5	11.8	61.2
3.5	20.1	17.1	4.9	9.8	46.1
4.4	27.6	29.2	9.9	11.7	21.5
4.6	29.9	30.4	10.7	11.6	17.4
5.0	23.9	43.0	11.3	6.1	15.7
6.8	12.4	—	29.0	27.5	31.1

have not exchanged with the solvent. Grzesiek et al. (6) found that some of them were not exchanged with solvent after 9 months. Worthy of note are the two very well-resolved signals of the C2H protons belonging to the H19 and H111 residues (Figure 8A,B), which undergo high-field shifts when these residues are deprotonated. These shifts during pH titration were used to measure the  $pK$  of both groups. High-field resonances (negative ppm) are no longer present in the spectra registered at high temperatures or pH 3.0, and the signals of the aromatic protons are also confined to a narrower field. The spectra under both conditions correlate well with what might be expected for an unfolded protein.

## DISCUSSION

Recombinant human  $\gamma$ -interferon gives an endotherm in DSC that is reversible over a relatively wide range of experimental conditions, which contrasts with the irreversible acid denaturation process reported by other authors (9, 18, 22). Arakawa et al. (19) found that the addition of NaCl to  $\gamma$ -interferon solutions induced the formation of aggregated species and decreased the refolding yields. We have confirmed this fact and found that the reversible pH window for thermal denaturation is narrower at higher buffer concentrations (see Table 1), probably because of an increase in ionic strength or sodium ions. The pH dependence of the amount of tertiary structure recovered after cooling was checked by fluorescence, biological activity, DSC (Table 1), CD (Figure 7 and Table 3), and  $^1H$  NMR (Figure 8) measurements, and all the results agreed satisfactorily. Arakawa et al. (19) write: "A major transition in tertiary structure of IFN- $\gamma$  occurs between pH 3.5 and pH 4.5, while much of the secondary structure still largely remains at pH 3.5 in the absence of NaCl. This remaining secondary structure is further partially destroyed by lowering the pH

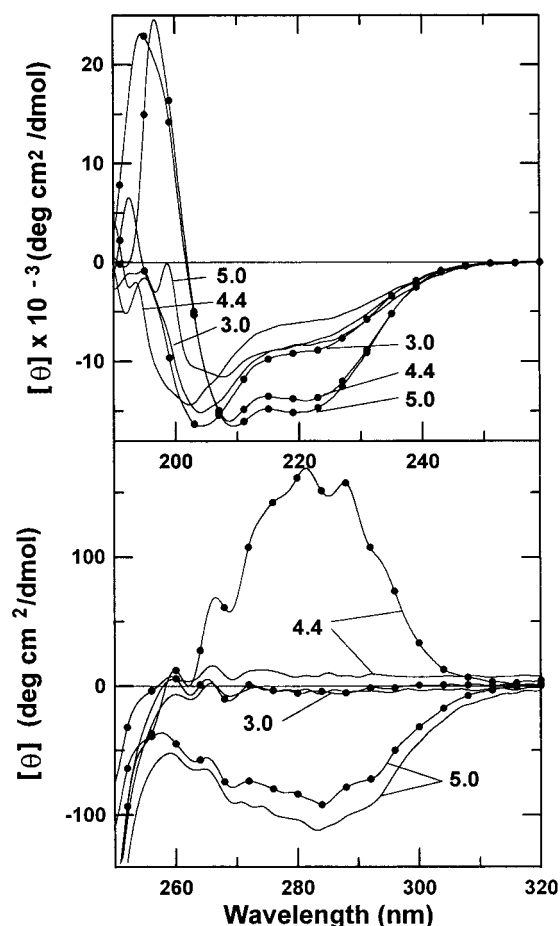


FIGURE 7: CD spectra of  $\gamma$ -interferon at the three pH values indicated. The spectra measured at 60 °C are the solid lines, and the spectra of the same heated samples after 2 h cooling and measured at 20 °C are the solid lines with black dots. Protein concentrations are the same as those in Figure 6.

to 2." Our results are very well described by this sentence, written more than 10 years ago on the basis of fewer experimental techniques. In Figure 6 two isosbestic points can be seen in the far-UV spectra, at about 208 and 205 nm, which coincides with those reported by Arakawa et al. (19).

Another important result of our study is our observation of the fact that the denaturation enthalpy depends on the buffer concentration in addition to the transition temperature.  $\Delta C_p$  is also a function of the buffer concentration (see Figure 3). The large and positive changes in the denaturation heat capacity of proteins are mainly due to the exposure to water of apolar groups previously buried in the native protein, partially offset by a negative contribution arising from the exposure of polar groups (41, 44). This hinders us from arriving at an unambiguous interpretation of the sharp decrease in  $\Delta C_p$  for  $\gamma$ -interferon with the increase in buffer concentration. Nevertheless, if we admit Chothia's observation (45) that the native globular proteins bury a constant proportion of their polar surface area and a variable proportion of their apolar surface area, the heat capacity changes would be correlated with the specific apolar contribution (for a fuller discussion, cf. refs 41, 46, and 47). We may conclude then that the number of hydrophobic groups of recombinant human  $\gamma$ -interferon exposed to the solvent by thermal denaturation decreases concomitantly with an increase in buffer concentration, perhaps due to higher aggregation,

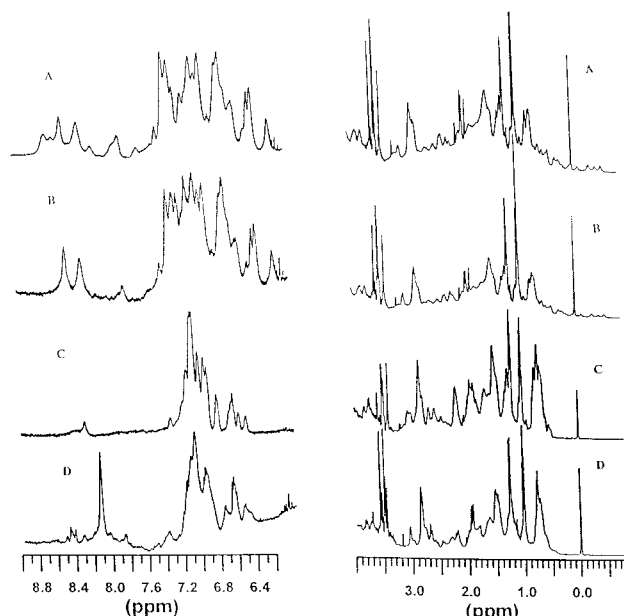


FIGURE 8:  $^1\text{H}$  NMR spectra of  $\gamma$ -interferon at pD 4.2 (A, B, and C) and 3.0 (D), in 5 mM sodium phosphate. Spectra A, C, and B were measured with the same sample at 25, 60, and 25  $^\circ\text{C}$  after cooling for 2 h, respectively. Spectrum D was measured at 25  $^\circ\text{C}$ . Protein concentrations were about 1.5 mg/mL.

which is ultimately responsible for the increase in irreversibility and also probably the reason for the lower stability of the protein at higher buffer concentrations.

The difference between the number of moles of protons stoichiometrically bound to a mole of protein in the thermally denatured and the native states,  $\Delta N^D$ , has been calculated, and the results are given in the inset of Figure 4. Two protons are bound to each protein-dimer molecule upon thermal denaturation at acid pH values, at which an amino acid residue of the protein with  $\text{pK} = 5.4$  is protonated, while there is no proton change when thermal denaturation takes place at basic pH values, with this residue unprotonated (see inset of Figure 4). This result appears to indicate that there is one unprotonated amino acid residue per monomer of native protein at pH 4, which is protonated upon thermal denaturation. This might mean that this group of the native protein has a higher  $\text{pK}$  value than that expected for normal protonation in water, probably due to its being buried inside the tertiary structure of the native protein. Aspartic or glutamic groups should therefore be the most promising candidates. There are 10 aspartic and 9 glutamic residues per protein monomer, and therefore it is not easy to find out exactly which residue is actually involved in the process. The dimer is around 34 000 daltons, and only the assignment of the chemical shifts of the backbone protons in its NMR spectrum has been published to date (6). With the knowledge of its X-ray structure, some of these residues can be eliminated, but the ambiguity is still not entirely resolved. It is worth noting that we did not observe any appreciable change in the structure of the native protein upon titrating this group with  $\text{pK}$  5.4 by CD (near- or far-UV), fluorescence, or  $^1\text{H}$  NMR in the aromatic region.

If we accept the existence of one amino acid residue with an abnormal  $\text{pK}$  value, the fact that the number of protons bound to the protein does not change upon thermal dena-

turation at neutral pH may be put down to either of the following two reasons: (a) the  $\text{pK}$  of this group is about this value of 5.4; or (b) the residue continues to be buried at neutral pH in the denatured protein because it is aggregated at this pH, implying that it is in the region responsible for the aggregation. Mulkerrin and Wetzel (22) showed that the aggregation is concomitant with the deprotonation of a group with a  $\text{pK}$  of 5.7, suggesting that one or two histidine residues may be involved in this process. Their experiments by chemical modification strongly suggest that at least one histidine is involved in this aggregation phenomenon, but the explanation may also lie in the deprotonation of some aspartic or glutamic acid residues interacting strongly with one or two of the histidines of the protein. Our measurements by  $^1\text{H}$  NMR indicate that the  $\text{pK}$  values of both histidines are 1 unit higher than this  $\text{pK}$  value. A  $\text{pK}$  of 6.4 for H111 was also reported by Lunn et al. (21). The region involved in the aggregation should be at the surface and relatively free. This fact, together with the probable implication of one or two histidine residues, lead us to believe that the loop connecting the A and B helices of  $\gamma$ -interferon may well be responsible for this aggregation. This loop (residues 18–28) is very flexible in free  $\gamma$ -interferon and undergoes a conformational change that includes the formation of a  $3_{10}$  helix upon receptor binding (7). The effect of metal ions and point mutations (48) and the X-ray results suggest that both histidines H19 and H111 are close to each other and form part of the binding surface on the  $\gamma$ -interferon molecule. If we accept as a working hypothesis that either the glutamic or the aspartic residue discussed above is interacting with one of these histidines, we might expect this acid residue to reside in the A, B, or F helices. Moreover, it should be buried, as was pointed out before. The only glutamic or aspartic residues to fulfill these conditions are E7, E9, and E112. Of these three residues, only the E112 residue exhibits a very low rate for the exchange of its NH proton with deuterium (6), and we believe that it could well be the amino acid residue with the abnormal protonation discussed above and that it may be responsible for the aggregation of the protein upon thermal denaturation. Nevertheless, it is widely accepted that the D21 residue has been preserved throughout evolution. It is also true that the mutation D24E (both groups are in the AB loop) induces an appreciable chemical shift in the H2 and H4 ring protons of H19 and H111 (48). These residues might then also be involved in these processes. Nevertheless, we think that it is better to go no further with these speculations until we have higher tertiary structure resolution or other physicochemical studies throw more light on the subject.

Finally, we would like to comment that we have significantly increased the yield of active dimer during the refolding of the protein after its denaturation by heat, acid, or urea, by a preliminary dialysis in 5 mM buffer at pH 4.5. After this dialysis, the protein was brought to neutrality with no additional loss of protein or activity.

## ACKNOWLEDGMENT

Our thanks go to Prof. Sánchez-Ruiz and Dr. Trout for their comments on the manuscript and to Dr. Filimonov for the Sigma-Plot programs.



## REFERENCES

1. Pestka, S., Langer, J., Zoon, K. C., and Samuel, C. E. (1987) *Annu. Rev. Biochem.* 56, 727–777.
2. Fountoulakis, M., Juranville, J. F., Maris, A., Ozmen, L., and Garotta, G. (1990) *J. Biol. Chem.* 265, 19758–19767.
3. Vijay-Kumar, S., Senadhi, S. E., Ealick, S. E., Nagabhushan, T., Trotta, P. P., Kosecki, R., Reichert, P., and Bugg, Ch. E. (1987) *J. Biol. Chem.* 262, 4804–4805.
4. Samuzdi, C. T., Burton, L. E., and Rubin, J. R. (1991) *J. Biol. Chem.* 266, 21791–21797.
5. Earlick, S. E., Cook, W. J., Vijay-Kumar, S., Carson, M., Nagabhushan, T. L., Trotta, P., and Bugg, Ch. (1991) *Science* 252, 698–702.
6. Grzesiek, S., Döbeli, H., Gentz, R., Garotta, G., Labhardt, A. M., and Bax, A. (1992) *Biochemistry* 31, 8180–8190.
7. Walter, M. R., Windsor, W. T., Tartanahalli, L. N., Lundell, D. J., Lunn, C. A., Zavodny, P. J., and Narula, S. K. (1995) *Nature* 376, 230–235.
8. Gray, P. W., Leung, D. W., Pennica, D., Yelverton, E., Najarian, R., Simonsen, C. C., Derynck, R., Sherwood, P. J., Wallace, D. M., Berger, S. L., Levinson, A. D., and Goeddel, D. V. (1982) *Nature* 295, 503–508.
9. Arakawa, T., Alton, N. K., and Hsu, Y. R. (1985) *J. Biol. Chem.* 260, 14435–14439.
10. Kung, H. F., Pan, Y. C. E., Moschera, J., Tsai, K., Bekesi, E., Chang, M., Sugino, H., and Honda, S. (1986) *Methods Enzymol.* 119, 204–210.
11. Perez, L., Vega, J., Chuay, C., Menendez, A., Ubieta, R., Montero, M., Padrón, G., Silva, A., Santizo, C., Besada, V., and Herrera, L. (1990) *Appl. Microbiol. Biotechnol.* 33, 429–434.
12. Zhang, Z., Tong, K. T., Belew, M., Petterson, T., and Janson, J. C. (1992) *J. Chromatogr.* 604, 143–155.
13. Rinderknecht, E., O'Connor, B. H., and Rodríguez, H. (1984) *J. Biol. Chem.* 259, 6790–6797.
14. Arakawa, T., Hsu, Y. R., Parker, C. G., and Lai, P. H. (1986) *J. Biol. Chem.* 261, 8534–8539.
15. Hogrefe, H. H., McPhie, P., Bekisz, J. B., Enterline, J. C., Dyer, D., Webb, D. S. A., Gerrard, T. L., and Zoon, K. C. (1989) *J. Biol. Chem.* 264, 12179–12186.
16. Pan, Y., Stern, A., Familletti, P., Khan, F., and Chizzonite, R. (1987) *Eur. J. Biochem.* 166, 145–149.
17. Lundell, D., Lunn, C. A., Dalgarno, A., Fossetta, J., Greenberg, R., Reim, R., Grace, M., and Narula, S. K. (1991) *Protein Eng.* 4, 335–341.
18. Hsu, Y. R., and Arakawa, T. (1985) *Biochemistry* 24, 7959–7963.
19. Arakawa, T., Hsu, Y. R., and Yphantis, D. A. (1987) *Biochemistry* 26, 5428–5432.
20. Lunn, C. A., Fossetta, J., Dalgarno, D., Murgolo, N., Windsor, W., Zavodny, P. J., Narula, S. K., and Lundell, D. (1992) *Protein Eng.* 5, 253–257.
21. Lunn, C. A., Fossetta, J., Murgolo, N., Zavodny, P. J., Lundell, D., and Narula, S. K. (1992) *Protein Eng.* 5, 249–252.
22. Mulkerrin, M., and Wetzel, R. (1989) *Biochemistry* 28, 6556–6561.
23. Gill, S. C., and von Hippel, P. H. (1989) *Anal. Chem.* 182, 319–326.
24. Makhatadze, G. I., Medvedkin, V. N., and Privalov, P. L. (1990) *Biopolymers* 30, 1001–1010.
25. Nisbet, I., Beilharz, M., Hertzog, P., Tymms, M., and Linnane, A. (1985) *Biochem. Int.* 11, 301–305.
26. Christensen, J. J., Hansen, L. D., and Izatt, R. M. (1976) *Handbook of Proton Ionization Heats and Related Thermodynamic Quantities*, John Wiley & Sons, New York.
27. Greenfield, N. J. (1996) *Anal. Biochem.* 23, 1–10.
28. Perczel, A., Park, K., and Fasman, G. D. (1992) *Anal. Biochem.* 203, 83–93.
29. Cortijo, M., Beldarrain, A., Molina, A. D., and Lopez-Lacomba, J. L. (1995) *Meas. Sci. Technol.* 6, 1086–1092.
30. Plaza del Pino, I. M., Pace, C. N., and Freire, E. (1992) *Biochemistry* 31, 11196–11202.
31. Davoodi, J., Wakarchuk, W. W., Surewicz, W. K., and Carey, P. R. (1998) *Protein Sci.* 7, 1538–1544.
32. Martinez, J. C., Viguera, A. R., Serrano, L., Filimonov, V. V., and Mateo, P. L. (1998) *React. Funct. Polymer.* 3, 221–225.
33. Plaza del Pino, I. M., and Sánchez-Ruiz, J. M. (1995) *Biochemistry* 34, 8621–8630.
34. Privalov, P. L. (1979) *Adv. Protein Chem.* 33, 167–241.
35. Privalov, P. L. (1982) *Adv. Protein Chem.* 35, 1–104.
36. Pfeil, W. (1986) in *Thermodynamic Data for Biochemistry and Biotechnology* (Hinz, H. J., Ed.) pp 349–376, Springer-Verlag, Berlin.
37. Hu, C. Q., Sturtevant, J. M., Thomson, J. A., Erickson, R. E., and Pace, C. N. (1992) *Biochemistry* 31, 4876–4882.
38. Genzor, C. G., Beldarrain, A., Gómez-Moreno, C., López-Lacomba, J. L., Cortijo, M., and Sancho, J. (1996) *Protein Sci.* 5, 1376–1388.
39. Ibarra-Molero, B., and Sánchez-Ruiz, J. M. (1996) *Biochemistry* 35, 14689–14702.
40. Dill, K. A. (1990) *Biochemistry* 29, 7133–7155.
41. Sánchez-Ruiz, J. M. (1995) in *Subcellular Biochemistry*, 24. *Proteins: Structure, Function and Engineering* (Biswas, B. B., and Roy, S., Eds.) pp 133–176, Plenum, New York.
42. Kern, G., Schülke, N., Schmid, F., and Jaenicke, R. (1992) *Protein Sci.* 2, 120–131.
43. Wang, C., Eufemi, M., Turano, C., and Giartosio, A. (1996) *Biochemistry* 35, 7299–7307.
44. Murphy, K. P., Bhakuni, V., Xie, D., and Freire, E. (1992) *J. Mol. Biol.* 227, 293–306.
45. Chothia, C. (1976) *J. Mol. Biol.* 105, 1–14.
46. Murphy, K. P., and Gill, S. J. (1991) *J. Mol. Biol.* 222, 699–709.
47. Murphy, K. P., and Freire, E. (1992) *Adv. Protein Chem.* 43, 313–361.
48. Lundell, D., Lunn, C. A., Senior, M. M., Zavodny, P. J., and Narula, S. K. (1994) *J. Biol. Chem.* 269, 16159–16162.

BI990287G